A Microstrip Antenna with Two U-Slots for Wi-Fi and 5G Applications

Dian Widi Astuti[1], Alya Patrakomala[2], Muslim Muslim[3], Said Attamimi[4], Dwi Astuti Cahyasiwi[5]

Abstract—**The development of telecommunications on wireless networks is advancing very rapidly. This rapid development is caused by the need for rapid information accessible from anywhere. One of the devices on the wireless network telecommunications system is an antenna. Antennas that can work on multiple wireless network frequencies on telecommunications system devices are indispensable. Therefore, this study proposes the design of a microstrip antenna capable of simultaneously working on two wireless network frequencies, namely Wi-Fi and fifth-generation cellular telecommunications (5G). The microstrip antenna was designed using two slots, i.e., the disconnected rectangular ring and inverted U-shaped slots. The Wi-Fi and 5G frequencies operating on this antenna were 2.45 GHz and 3.3 GHz. The microstrip antenna resonant frequency was affected by the slot length. The antenna was designed and fabricated using a Rogers 5880 substrate with a material's relative permittivity (ε_r) of 2.2, a tangent loss (δ) of 0.0009, and a thickness of 1.575 mm. Before being fabricated, the antenna design was simulated using the Ansys HFSS simulator, which is a simulator for designing components using electromagnetic waves including antennas. Compared to the simulation results, the results of reflection coefficient measurement in this antenna design showed excellent results for both frequencies. In the simulation results, the reflection coefficient provided a bandwidth of 123 MHz in the 2,412–2,535 MHz frequency range, while the measurement results provided a bandwidth value of 153 MHz in the 2,402–2,555 MHz frequency range for the Wi-Fi frequency application. At the 5G frequency, a measuring bandwidth of 87 MHz was obtained in the range of 3,260–3,347 MHz. The measurement results were commensurate with the simulation results, which obtained a bandwidth of 88 MHz in the range of 3,248-3,336 MHz. Therefore, the fabrication of this antenna design can be used for both applications.**

Keywords—**Microstrip Antenna, Dual-Band Antennas, Wi-Fi, 5G Antenna, Two Slots.**

I. INTRODUCTION

In today's era of globalization, the use of telecommunication networks is advancing very rapidly, especially wireless telecommunication networks such as Wi-Fi and the fifth-generation mobile network (5G) [1]. It is because Wi-Fi and 5G networks provide ease of information dissemination. Therefore, it takes an antenna device to establish such a wireless network. One of the needs of future applications of wireless communication systems is an antenna with multifrequency capabilities. The multi-band antenna has two or more resonant frequencies so that the effectiveness of a single antenna device can be maximized. Another advantage of multifrequency antennas is reducing the cost and dimensions of a device system because one antenna can be used for various applications.

An antenna is a device that can operate as a transmitter and receiver of electromagnetic waves emitted through a transmission medium in the form of free air. Therefore, the antenna is also called a transceiver component placed at the end or beginning (front-end) of the wireless telecommunication system. The realization of the antenna can be carried out using a substrate material known as a microstrip antenna [2]-[4], a metal material such as a waveguide antenna [5], a wire material such as a dipole antenna [6], and others.

Microstrip antennas are easily fabricated compared to other materials [7]. In addition, multifrequency-microstrip antennas provide simpler dimensions compared to single-frequency antennas. Various studies on methods for generating antennas with two or more resonant frequencies have been conducted. Reference [4] has conducted multi-band antenna research using two substrates stacked into one and input with one port. The lower substrate had a branched unification structure as well as the addition of stub channels for the matching process. On the upper layer of the substrate, there was a tooth-shaped radiation element. The antenna design was applied to Wi-Fi, 5G, and other wireless applications. This study provides fairly suitable results between simulation and measurement.

Reference [8] realized a microstrip antenna operating at two frequencies using two rectangular slots. Each rectangular slot in [8] worked for a different frequency. The research has succeeded in providing good stopband characteristics. Then, the shape of the rectangular slot could be modified into a barbell-shaped slot with a hollow circle in the middle [9]. The dual-band antenna in this study operated at a center frequency of 9.5 GHz and 13.85 GHz. Similar to [8], this study also used different transverse electric (TE) modes for each resonance frequency [9]. Reference [10] made the rectangular slots transverse to each other resulting in dual-band operated at 2.47 GHz and 3.59 GHz. All of the previously mentioned studies can produce a two-frequency microstrip antenna using substrate-integrated waveguide (SIW) technology. However, the design obtained 5% fractional bandwidth (FBW) measurement, which was still very narrow [8]-[10].

[1,2,3,4] *Electrical Engineering Study Program, Mercu Buana University-Jakarta, Jl Meruya Selatan No. 1 Jakarta Barat 11650 INDONESIA (tel.: 021-5840 816; fax: 021-5871 335; email: [1]dian.widiastuti@mercubuana.ac.id, [2]putri.alyapatrakomala@gmail.com, [3]muslim@mercubuana.ac.id, [4]said.attamimi@mercubuana.ac.id)*

[5] *Electrical Engineering Study Program, Universitas Muhammadiyah Prof. Dr. HAMKA, Jl. Tanah Merdeka No.6, RW.5, Rambutan, Kec. Ciracas, East Jakarta, 13830 (email: [5]dwi.cahyasiwi@uhamka.ac.id)*

[Received: 24 February 2022, Revised: 10 October 2022]

References [11] and [12] employed rectangular slots bent like a river (meander), resulting in a dual-band microstrip antenna. Reference [11] applied antennas operating at frequencies of 900 MHz and 2,450 MHz. Another dual-band antenna study used various slot shapes ranging from irregular triangles, two slots on the top and bottom of the substrate, two stacked isosceles triangle slots, circular slots, and others to produce two to three resonant frequencies [13]-[18]. However, the given FBW in [18] was less than 3%. It is due to the small antenna dimensions, which use an eighth mode substrate integrated waveguide (EMSIW) structure due to a miniaturization factor (MF) of 87.5%.

References [19] and [20] used rectangular slots bent into a U letter to producing two to three frequencies. Both studies managed to provide the same measurement results as the simulation results [19], [20]. However, the maximum value of the resulting simulated FBW was 6.9% [20]. In addition, the fabrication of such an antenna is relatively complicated because it uses two substrates hanging from each other by being separated by an air layer.

Another dual-band microstrip antenna study used an L-shaped slot [21]. The letter L comes from a separate U with a certain gap. The antenna works at a center frequency of 2.45 GHz and 5.8 GHz, with FBW frequency measurement results of 2.57% and 2.58%. However, this study still has a narrow FBW below 3% [21]. Other rectangular-shaped microstrip antenna studies have also been conducted [22], [23]. Reference [22] designed a simple square microstrip antenna working at a frequency of 3.3 GHz with Momentum on the Advance Design System (ADS). However, the antenna design was not fabricated. Meanwhile, another study produced 45° polarizations using two interdigital resonators [23]. The study resulted in an FBW of 6.45% with excellent selectivity. It was due to the presence of an integrated filter set into one so that the antenna gained response resembled a bandpass filter. However, the resulting resonance frequency was only one piece for 5G applications at a frequency of 4.65 GHz. Therefore, this study proposes a dual-band microstrip antenna using disconnected square ring-shaped and inverted U-shaped slots. This study aims to generate an FBW antenna with a more than 5% measurement and smaller antenna dimensions. The antenna was implemented on Wi-Fi and 5G frequency applications. The selected Wi-Fi application was at a center frequency of 2.45 GHz, while the 5G frequency was at a center frequency of 3.3 GHz based on [24]. Although 5G technology in Indonesia does not use the 3.3 GHz center frequency due to the effects of humidity [24], 5G technology that uses the 3.3 GHz center frequency is applicable in other countries, such as the United States [25].

This microstrip antenna was fabricated using Rogers Duroid RO 5880 substrate material which could be obtained on the market. The writing of this study began by producing the antenna design discussed in Section II, the fabrication and measurement of the antenna discussed in Section III, and ended with the conclusion in Section IV.

II. ANTENNA DESIGN

Microstrip antenna design with a disconnected square ring-shaped slot and inverted U-shaped slot for Wi-Fi and 5G

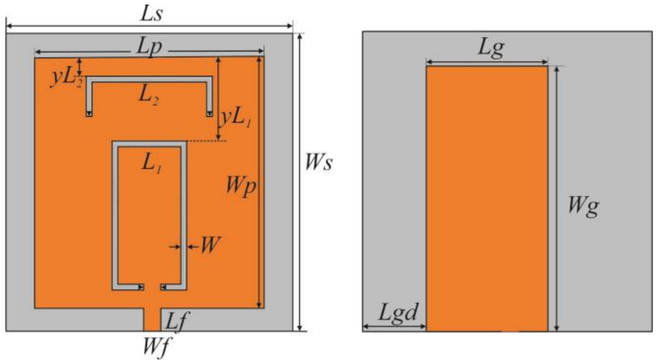

(a) (b)

Fig. 1 Schematic figure antenna: (a) top view, (b) bottom view.

TABLE I
ANTENNA DIMENSIONS

Parameters	Value (mm)	Parameters	Value (mm)	Parameters	Value (mm)
Ls	50	*Ws*	52.0	*Lp*	40.0
Wp	44	L_1	71.0	L_2	34.0
Lf	4	yL_1	14.8	yL_2	3.5
W	1	*Wf*	3.0	*Lg*	21.0
Wg	46	*Lgd*	11.0		

applications are shown in Fig. 1, while antenna dimension is shown in Table I. The antenna design began with the antenna's resonance frequency selection. This frequency selection would affect the dimensions of the antenna used. The higher the working frequency of the antenna was, the smaller the dimension of the antenna was, and vice versa. Measurements of antenna magnitudes, such as reflection coefficient parameters, shifts in impedance bandwidth, gain, radiation pattern, axial ratio, antenna efficiency, and others, were also influenced by the selection of substrate materials.

A. *Antenna Substrate*

The selection of the substrate material significantly affected the performance of the reflection coefficient parameters of the microstrip antenna. Therefore, selecting substrates with small tangent losses were considered in the selection of substrates. This antenna design used a Rogers Duroid 5880, substrate, with a tangent loss of 0.0009, a relative permittivity (ε_r) of 2.2, with a substrate thickness (h) of 1.575 mm. The selection of substrates with small tangent losses aimed to minimize losses, while the selection of thick substrates aimed to allow electromagnetic waves from the slot to radiate out maximally. In addition, a substrate with a relatively small material permittivity should be used in the design of antennas.

B. *Antenna Dimensions*

The dimensions of the rectangular-shaped antenna patch comprised a (W_p) width and (L_p) length. The patch width (W_p) can be calculated by the formula (1) [21].

$$W_p = \frac{c}{2f_r}\sqrt{\frac{2}{\varepsilon_r+1}}. \quad (1)$$

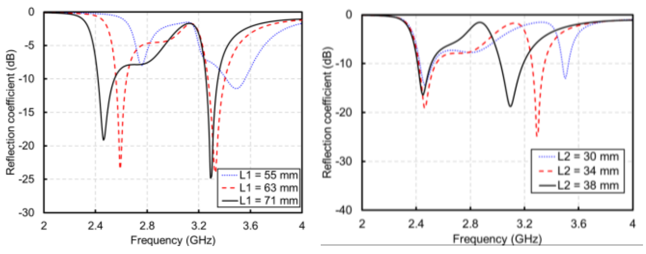

(a) (b)

Fig. 2 Reflection coefficient simulation of the length parameter for (a) $L1$ slot, and (b) slot $L2$ with other parameters fixed.

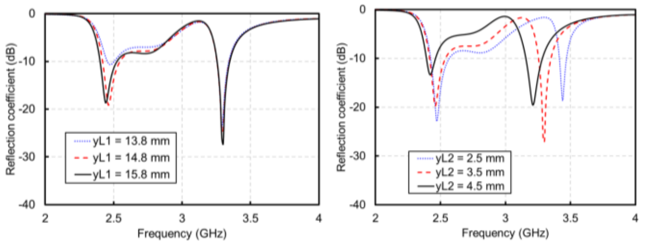

(a) (b)

Fig. 3 Reflection coefficient simulation of the slot position parameter for (a) $yL1$, and (b) $yL2$ with other parameters fixed.

Given the value of ε_r = 2.2, the center frequency of the antenna design, f_r = 2.45 GHz, and the speed of the light, c = 3 × 10^8 m/s, W_p is obtained using the following formula approach:

$$W_p = \frac{3\times10^8}{2\cdot2.45\cdot10^9}\sqrt{\frac{2}{2.2+1}} = 48.40 \text{ mm}.$$

Since $W_p/h > 1$, effective values of (ε_{reff}) relative permittivity, (ΔL) delta length, (L_{eff}), and L_p effective lengths could be calculated using (2)-(5) [21].

$$\varepsilon_{reff} = \frac{\varepsilon_r+1}{2} + \frac{\varepsilon_r-1}{2}\left[1+12\frac{h}{W_p}\right]^{-1/2} \quad (2)$$

$$\Delta L = h\cdot 0.412\frac{(\varepsilon_{reff}+0.3)\cdot\left(\frac{W_p}{h}+0.264\right)}{(\varepsilon_{reff}-0.258)\cdot\left(\frac{W_p}{h}+0.8\right)} \quad (3)$$

$$L_{eff} = \frac{c}{2\cdot f_r\sqrt{\varepsilon_{reff}}} \quad (4)$$

$$L_p = L_{eff} - 2\cdot\Delta L. \quad (5)$$

From (2)-(5), the values of ε_{reff} = 2.11, ΔL = 0.83 mm, L_{eff} = 42.16 mm, and L_p = 40.5 mm could be obtained. Subsequently, the antenna design was optimized with Ansys HFSS to obtain optimal results according to the target.

Two slots were added in rectangular patch radiators to emit electromagnetic waves into the air. The first slot was a disconnected rectangular ring with the overall length of the slot being L_1 and the second slot was an inverted U-shaped with a total length of L_2. The disconnected rectangular ring slot was placed at a distance of 14.5 mm from the top edge of the square patch, while the inverted U slot was placed at a distance of 3.5 mm. Both slots were made on a rectangular radiator with L_p = 44 mm and W_p = 40 mm, which was the result of the optimization of the above calculations. On the radiator, a rectangular patch was connected with a 50 Ω transmission line which was 4 mm long and 3 mm wide as a current input. The entire antenna structure was printed on a 50 mm × 52 mm substrate. On the back of the antenna, not all substrate layers were filled with a copper layer as ground. However, some of the ground layers were peeled off for the optimization process to obtain a reflection coefficient of -10 dB and expand the impedance bandwidth. From optimization results, the length and width of the ground were 21 mm and 46 mm, respectively, and were located at a distance of 11 mm from the left edge of the ground. The optimization results of the antenna design are shown in Fig. 1.

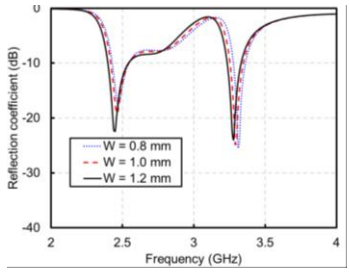

Fig. 4 Reflection coefficient simulation of the slot thickness parameter (W) with other parameters fixed.

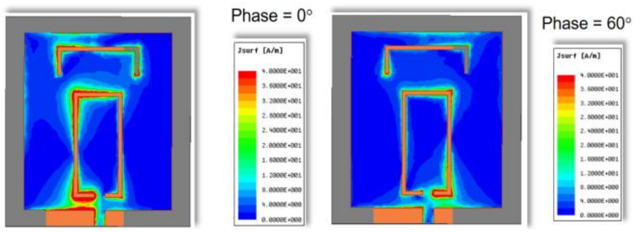

(a) (b)

Fig. 5 Surface current flow of 2.45 GHz frequency on phase (a) 0°, (b) 60°.

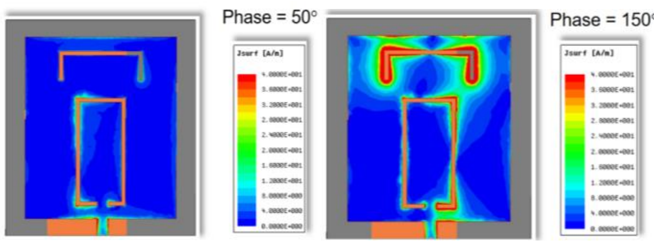

(a) (b)

Fig. 6 Surface current flow of 3.3 GHz frequency on phase, (a) 50°, (b) 150°.

C. *Parameters Study*

Fig. 2 shows the results of parameter studies for low frequency (f_1) and high frequency (f_2). The frequency f_1 was at 2.45 GHz, while f_2 was at 3.3 GHz. Fig. 2 shows that f_1 is more affected by the length parameter of the L_1 slot, i.e., the longer L_1, the f_1 shifts to a lower frequency. It also applies to the reverse. At high frequencies, f_2 was more affected by the L_2 length parameter, i.e., the shorter L_2, the frequency f_2 shifted to a frequency higher than the previous frequency. Therefore, the length parameter of both slots was set to obtain a frequency corresponding to the target.

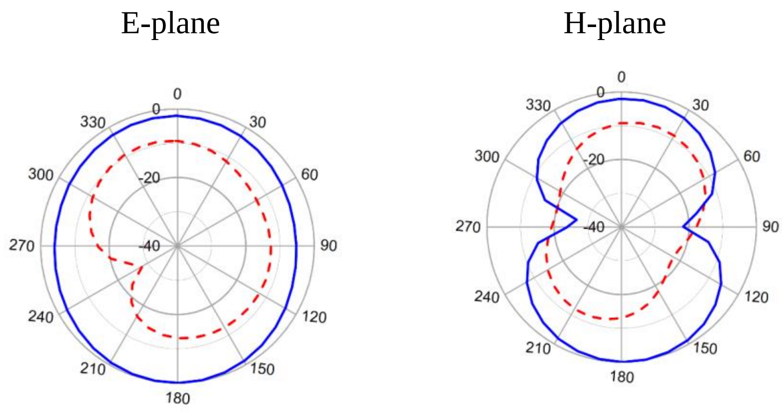

(a)

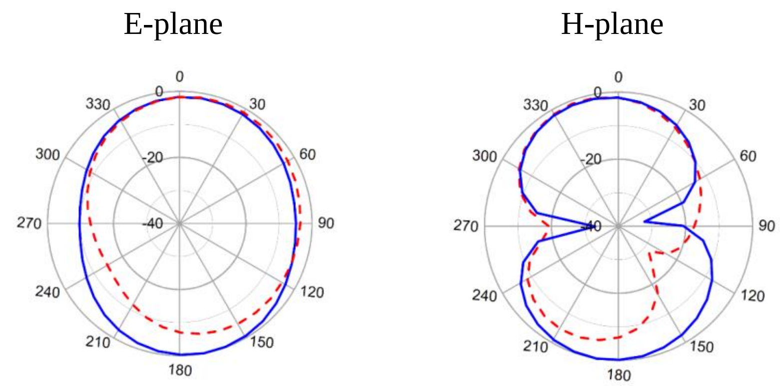

(b)

Fig. 7 Radiation pattern simulation for E-plane and H-plane on (a) 2.45 GHz, and (b) 3.3 GHz; the red dash line for cross-polarization, while the blue solid line for co-polarization.

Fig. 3 shows a parameter study of yL_1 and yL_2 slot positions. The change in the value of the reflection coefficient from f_1 was more influenced by the position of the L_1 slot alone, as shown in Fig. 3(a). The further up the position of slot L_1, the f_1 experiences a loss of matching condition, as shown by the blue dotted line curve. The further down the position of the slot L_1, the better the matching condition for the resonance frequency f_1, as shown by the intact black line curve. The study result of yL_1 optimum value was 1.2 mm. Fig. 3(b) shows the change in the position of slot L_2, which affects the resonance frequency shift in f_1 and f_2. The rise in the position of the slot L_2 resulted in a shift of the resonance frequencies, both f_1 and f_2, towards a higher resonance frequency than before. It was reversed if the position of slot L_2 was in a position close to slot L_1.

Fig. 4 shows the simulation of the parameter against the W slot thickness. The reduced value of W caused a shift of the resonant frequencies f_1 and f_2 to a higher frequency than the previous frequency. When the slot was thickened, there was a shift of the resonant frequencies f_1 and f_2 to a lower frequency. The change in the slot thickness parameter did not significantly change the reflection coefficient parameter compared to the change in the parameters L_1, L_2, and the slot positions yL_1 and yL_2. The selection of L_1, L_2, yL_1, yL_2, and W values was based on the results of reflection coefficient parameters following the dual band antenna configuration design. The optimization results of the antenna design are shown in Table I.

D. Surface Current Flow

Fig. 5 shows a simulation of surface current flow on the design of antennas working at 2.45 GHz frequency. This simulation of surface current flow is necessary to determine the part of the antenna that emits electromagnetic waves into the free air. The strength of the value of the surface current parameter is demonstrated by color degradation. Color degradation from blue to red reveals strong surface currents that flow from weak strength to great strength. The same scale of surface current flow was used to detect the same strength of surface current flow across both frequencies. The scale of surface current flow in the design was 40 A/m. Fig. 5(a) shows that the antenna has an emission at the right of the antenna at slot L_1 in phase 0°, while in Fig. 5(b), it appears that the emission of surface current flow is present in phase 60°. In that phase, it is seen that the antenna has a surface current flow emission in the left-hand part of the slot L_1. It relates to the radiation pattern of the antenna design.

 p-ISSN 2301 – 4156 | e-ISSN 2460 – 5719

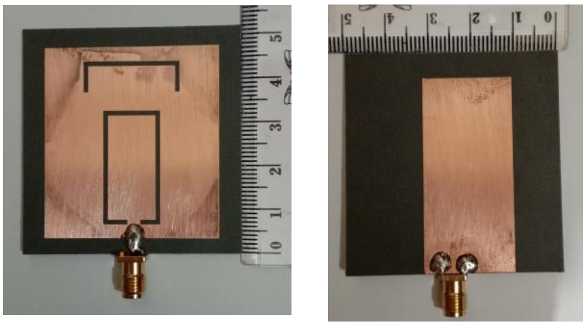

(a) (b)

Fig. 8 Antenna fabrication for (a) the top view, and (b) the bottom view.

The simulation of surface current flow at a higher frequency, i.e., 3.3 GHz, is in slot L_2, as shown in Fig. 6. In Fig. 6(a), surface current flow occurs in phase 50° with minimal surface current flow. Such a small surface current flow occurs on the right and left sides of the slot L_2. Fig. 6(b) shows the maximum surface current flow occuring on the right and left sides of the $L2_{slot}$. The maximum surface current flow occurs in phase 150°.

E. Radiation Patterns

Fig. 7(a) shows the simulation results of the radiation pattern at a frequency of 2.45 GHz in the omnidirectional form for the E plane, with a cross-polarization discriminant (XPD) of about 6.5 dB and a maximum amplification direction of 2 dBi at theta 180°. As the type of omnidirectional radiation pattern, then as shown in Fig. 7(a) on the right, in the H plane, the radiation pattern at the frequency of 2.45 GHz is shown in two amplification directions of 1 dBi and 2 dBi in the direction of theta 0° and 180°, respectively. The XPD in both directions is between about 7 dBi and 13 dBi.

Fig. 7(b) on the left shows the radiation pattern at a frequency of 3.3 GHz, which is also omnidirectional, with a maximum amplification direction at theta 170° of 1.5 dBi and XPD of 6 dB in the E plane. The radiation pattern at a frequency of 3.3 GHz in the H plane shows two directions of amplification at theta -15° and 180° with magnitudes of 0 dB and 1 dB, respectively. An XPD of 7 dB was obtained in the 180° direction. The omnidirectional radiation pattern at both frequencies was caused by the partial grounding of this antenna design.

III. Fabrication and Measurement

Fig. 8 shows the results of microstrip antenna fabrication using the photo etching process. The photo etching process facilitates the fabrication of microstrip antennas compared to other antenna types. Fig. 8(a) shows the upper part of the antenna with the slot of the transmitting or irradiating part, while Fig. 8(b) shows the lower part of the antenna.

The prefabricated antenna needs to be tested for performance. One of the antenna performance test parameters is the reflection coefficient measurement parameter, in addition to measuring the antenna radiation pattern, gain, efficiency, and others. The measurement results of the antenna reflection coefficient

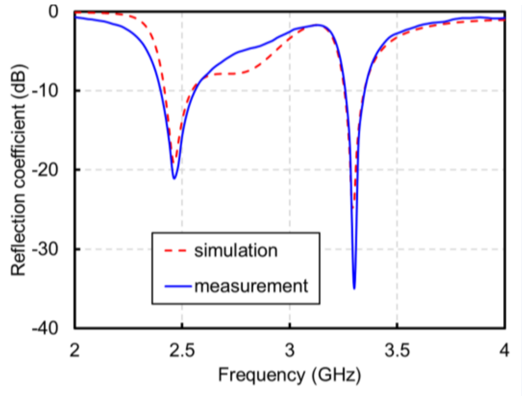

Fig. 9 Reflection coefficient simulation result in the red dash line while the reflection coefficient measurement result in the blue solid line.

TABLE II
COMPARISON WITH PREVIOUS RESEARCH

Reference	Antenna Type	Frequency f_1/f_2 (GHz)	Substrate Dimension $l \times w \times h$ (λ_0^3)	FBW on f_1 (%)	FBW on f_2 (%)
[9]	SIW	9.5/13.85	0.82×1.17×0.02	1.820	1.44
[10]	SIW	2.47/3.59	10.49×11.54×0.06	0.486	0.78
[21]	MPA	2.45/5.8	4.9×3.67×0.08	2.570	2.58
This Work	Dual U-slot	2.45/3.3	6.12×6.37×0.14	6.170	2.63

parameters as a result of fabrication are shown in Fig. 9. Simulation results are shown in red dashed lines, while measurement results are shown in whole blue lines. The simulation results of the reflection coefficient at the level of -10 dB in the first resonance gave a bandwidth of 123 MHz (2,412–2,535 MHz), while a bandwidth of 153 Mhz (2,402–2,555 MHz) was obtained from the measurement. It can be seen that the measurement results are 25% wider than the simulation results and shift by 20 MHz towards higher frequencies. At the second resonance frequency, for a reflection coefficient level of -10 dB, a measurement impedance bandwidth of 87 MHz (3,260–3,347 MHz) was obtained. The impedance bandwidth was rather commensurate with the simulation results, i.e., 88 MHz, which was in the frequency range of 3,248–3,336 MHz. There was a difference in measurement results, i.e., the resonance frequency showed a 3% shift towards higher frequencies. The reflection coefficient measurement results showed a very suitable comparison for simulation. It was shown by the impact of measurement results with simulation results on the working frequency of the antenna. The simulated FBW was 5% for f_1 and 2.67% for f_2). The FBW measurement results were 6.17% and 2.63% at a center frequency of 2.47 and 3.3 GHz.

The lowest reflection coefficient value at low frequencies was -19 dB, while the measurement results showed a smaller value, namely -21 dB. The high-frequency reflection coefficient measurement results also showed a smaller value of 10 dB compared to the simulation, which was from -24 dB to -34 dB. Fig. 9 shows the difference in depth or small value of the reflection coefficient. It is more caused by the process of soldering the connector, causing a difference in the input impedance value of the current input channel. Measurement of other antenna parameters, such as radiation pattern, gain, and antenna efficiency, was not done because there was an improvement in anechoic chamber room facilities.

Table II shows the comparison of the results of this study with previous studies. Table II shows that the microstrip antenna design with disconnected rectangular ring-shaped and inverted U-shaped slots has greater FBW measurement results compared to previous studies [9], [10], [21]. Such greater FBW measurement results apply to f_1 and f_2. The antenna used was a SIW microstrip [9], [10], and a regular microstrip patch with four L-shaped slots [21]. This study has the dimensions of an antenna with a smaller total volume compared to the study in [10].

IV. Conclusion

The dual-band microstrip antennas with a disconnected rectangular ring and inverted U slots were fabricated using Rogers Duroid 5880 substrate with a thickness of 1.575 mm. The measurement results of the reflection coefficient showed excellent results compared to the simulation results at the frequency of 2.47 GHz and 3.3 GHz. At a center frequency of 2.47 GHz, the results of FBW simulation of antenna design were obtained by 5% (2,412–2,535 MHz), while the measurement results were obtained by 61.7% (2,402–2,555 MHz). At a center frequency of 3.3 GHz, the FBW simulation results were 2.67% (3,260–3,347 MHz), while the measurement results were 2.63% (3,260–3,347 MHz). Although FBW at high frequencies is less than 5%, the measurement bandwidth is still commensurate with the 5G application. The frequencies of this antenna design can be applied to Wi-Fi and 5G wireless frequencies.

Conflict of Interest

The author states that there is no conflict of interest with any party from the beginning to the end of the study.

Author Contribution

Dian Widi Astuti and Said Attamimi were responsible for conceptualization, article draft writing, corresponding authors, and supervision of all research until publication of the article; Alya Patrakomala was in charge of the simulation data operator on HFSS software and the antenna design fabrication commensurate with the research objectives; Muslim assisted with the antenna fabrication and measurement, Dwi Astuti Cahyasiwi contributed as a data analyst of simulation and measurement findings.

Acknowledgment

The authors acknowledge Mr. Bagus Edi Sukoco for his assistance during the antenna measuring procedure at the National Research and Innovation Agency (BRIN), Bandung. Gratitudes are also given to the JNTETI Team and reviewers for taking the time to make this article better.

References

[1] Ericsson, "Harnessing the 5G Consumer Potential: The Consumer Revenue Opportunity Uncovered," 2020, [Online], https://www.ericsson.com/en/reports-andpapers/consumerlab/reports /harnessing-the-5g-consumer-potential, access date: 20-Jul-2022.

[2] J. Prasojo and D. Widiastuti, "Rectangular Microstrip Antenna with Annular Slot for WLAN," *Int. Conf. Broadband Commun. Wirel. Sensors, Powering (BCWSP)*, 2017, pp. 1–5.

[3] D.W. Astuti and E.T. Rahardjo, "Size Reduction of Substrate Integrated Waveguide Cavity Backed U-Slot Antenna," *2018 IEEE Indian Conf. Antennas, Propag. (InCAP)*, 2018, pp. 1–4.

[4] D.W. Astuti, A. Firdausi, and M. Alaydrus, "Multiband Double Layered Microstrip Antenna by Proximity Coupling for Wireless Applications," *QiR 2017 - 2017 15th Int. Conf. Qual. Res. (QiR): Int. Symp. Elect., Comput. Eng.*, 2017, pp. 106–109.

[5] Y. Rao, H. Zhang, and G. Sun, "Shared Aperture Dual-Band Waveguide Slot Antenna," *2020 IEEE Int. Symp. Antennas, Propag., North Amer. Radio Sci. Meeting (IEEECONF 2020)*, 2020, pp. 693–694.

[6] J.D. Hawkins, L.B. Lok, P.V. Brennan, and K.W. Nicholls, "HF Wire-Mesh Dipole Antennas for Broadband Ice-Penetrating Radar," *IEEE Antennas Wirel. Propag. Lett.*, Vol. 19, No. 12, pp. 2172–2176, Dec. 2020.

[7] L. Xiang, Y. Zhang, Y. Yu, and W. Hong, "Characterization and Design of Wideband Penta- and Hepta-Resonance SIW Elliptical Cavity-Backed Slot Antennas," *IEEE Access*, Vol. 8, pp. 111987–111994, Jun. 2020.

[8] B.-J. Niu, J.-H. Tan, and C.-L. He, "SIW Cavity-Backed Dual-Band Antenna with Good Stopband Characteristics," *Electron. Lett.*, Vol. 54, No. 22, pp. 1259–1260, Nov. 2018.

[9] S. Mukherjee *et al*., "Substrate Integrated Waveguide Cavity-Backed Dumbbell-Shaped Slot Antenna for Dual-Frequency Applications," *IEEE Antennas Wirel. Propag. Lett.*, Vol. 14, pp. 1314–1317, Dec. 2014.

[10] K. Yoshihara, M. Tamura, Y. Miyaji, and A. Alphones, "Dual Band SIW Cavity-Backed Crossed-Slot Antenna," *Asia-Pac. Microw. Conf. Proc. (APMC)*, 2019, pp. 1539–1541.

[11] A. Ghaffar *et al*., "A Compact Dual-Band Flexible Antenna for Applications at 900 and 2450 MHz," *Prog. Electromagn. Res. Lett.*, Vol. 99, pp. 83–91, May 2021.

[12] J.H. Lu and H.S. Huang, "Planar Compact Dual-Band Monopole Antenna with Circular Polarization for WLAN Applications," *Int. J. Microw., Wirel. Technol.*, Vol. 8, No. 1, pp. 81–87, Feb. 2016.

[13] K. Mahendran, D.R. Gayathri, and H. Sudarsan, "Design of Multi Band Triangular Microstrip Patch Antenna with Triangular Split Ring Resonator for S Band, C Band and X Band Applications," *Microprocess. Microsyst.*, Vol. 80, pp. 1–9, Feb. 2021.

[14] T. Wattakeekamthorn, K. Wattakeekamthorn, C. Mahatthanajatuphat, and P. Akkaraekthalin, "Dual-Bands Operation Base on an Asymmetrical Double Triangular Slot Fed by CPW with Stair-Step for WLAN 2.45 GHz and 5.5 GHz," *Proc. 2021 9th Int. Elect. Eng. Congr. (iEECON)*, 2021, pp. 527–530.

[15] M.C. Jose *et al.*, "Compact Dual-Band Millimeter-Wave Antenna for 5G WLAN," *Int. J. Microw., Wirel. Technol.*, Vol. 14, No. 8, pp. 981–988, Oct. 2022.

[16] W. Luo, W. Chen, Y. Ren, and M. Wang, "Dual-Band and Dual Circularly Polarized Sequential Rotation Antenna Array for Vehicle Satellite Communications," *Electromagn.*, Vol. 42, No. 1, pp. 51–65, Apr. 2022.

[17] G. Liu, C. Zhang, Z. Chen, and B. Chen, "A Compact Dual Band MIMO Antenna for 5G/WLAN Applications," *Int. J. Microw., Wirel. Technol.*, to be published.

[18] M. Mujumdar and A. Alphones, "Eighth Mode Substrate Integrated Waveguide Dual Band Resonator Antennas," *IET Microw. Antennas, Propag.*, Vol. 11, No. 9, pp. 1262–1266, Jul. 2017.

[19] H. Lu, Y. Liu, F. Liu, and W. Wang, "Single-Feed Single-Patch Triple-Band Single-Beam/Dual-Beam U-Slotted Patch Antenna," *Prog. Electromagn. Res. M*, Vol. 77, pp. 17–28, 2019.

[20] W.C. Mok, S.H. Wong, K.M. Luk, and K.F. Lee, "Single-Layer Single-Patch Dual-Band and Triple-Band Patch Antennas," *IEEE Trans. Antennas Propag.*, Vol. 61, No. 8, pp. 4341–4344, Aug. 2013.

[21] S. Ahmad, A. Ghaffar, N. Hussain, and N. Kim, "Compact Dual-Band Antenna with Paired L-Shape Slots for On-and Off-Body Wireless Communication," *Sensors*, Vol. 21, No. 23, pp. 1–16, Nov. 2021.

[22] I. Hossain, T. Ahmed, and H. Kabir, “Design of Rectangular Microstrip Patch Antenna at 3.3 GHz Frequency for S-band Applications,” *Int. J. Eng., Manuf.*, Vol. 12, No. 4, pp. 46–52, Aug. 2022.

[23] D.A. Cahyasiwi, F.Y. Zulkifli, and E.T. Rahardjo, “Switchable Slant Polarization Filtering Antenna Using Two Inverted Resonator Structures for 5G Application,” *IEEE Access*, Vol. 8, pp. 224033–224043, Dec. 2020.

[24] W.R. Dyah, K. Anwar, and L.O. Nur, “Humidity Effect to the Indonesia 5G Channel Model at 3.3 GHz,” *2019 Symp. Future Telecommun. Technol. (SOFTT)*, 2019, pp. 1–5.

[25] (2020) “5G Frequency Bands & Spectrum Allocations,” [Online], https://www.cablefree.net/wirelesstechnology/4glte/5g-frequency-bands-lte/, access date: 07-Oct-2022.